Physiol Genomics 26: 180–191, 2006.
First published May 2, 2006; doi:10.1152/physiolgenomics.00029.2005.

Nox2-containing NADPH oxidase and Akt activation play a key role in angiotensin II-induced cardiomyocyte hypertrophy

Shawn D. Hingtgen,[1] Xin Tian,[1] Jusan Yang,[1] Shannon M. Dunlay,[1] Andrew S. Peek,[6] Yihe Wu,[6] Ram V. Sharma,[1,3] John F. Engelhardt,[1,2,3,4,5] and Robin L. Davisson[1,2,3,4]

[1]*Department of Anatomy and Cell Biology, The Free Radical and Radiation Biology Program,* [2]*Department of Radiation Oncology,* [3]*The Cardiovascular Center,* [4]*The Center for Gene Therapy of Cystic Fibrosis and Other Genetic Diseases, and* [5]*Department of Internal Medicine, Roy J. and Lucille A. Carver College of Medicine, The University of Iowa, Iowa City; and* [6]*Integrated DNA Technologies, Coralville, Iowa*

Submitted 27 January 2005; accepted in final form 24 April 2006

Hingtgen, Shawn D., Xin Tian, Jusan Yang, Shannon M. Dunlay, Andrew S. Peek, Yihe Wu, Ram V. Sharma, John F. Engelhardt, and Robin L. Davisson. Nox2-containing NADPH oxidase and Akt activation play a key role in angiotensin II-induced cardiomyocyte hypertrophy. *Physiol Genomics* 26: 180–191, 2006. First published May 2, 2006; doi:10.1152/physiolgenomics.00029.2005.—Angiotensin II (ANG II) has profound effects on the development and progression of pathological cardiac hypertrophy; however, the intracellular signaling mechanisms are not fully understood. In this study, we used genetic tools to test the hypothesis that increased formation of superoxide ($O_2^-\cdot$) radicals from a Rac1-regulated Nox2-containing NADPH oxidase is a key upstream mediator of ANG II-induced activation of serine-threonine kinase Akt, and that this signaling cascade plays a crucial role in ANG II-dependent cardiomyocyte hypertrophy. ANG II caused a significant time-dependent increase in Rac1 activation and $O_2^-\cdot$ production in primary neonatal rat cardiomyocytes, and these responses were abolished by adenoviral (Ad)-mediated expression of a dominant-negative Rac1 (AdN17Rac1) or cytoplasmic Cu/ZnSOD (AdCu/ZnSOD). Moreover, both AdN17Rac1 and AdCu/ZnSOD significantly attenuated ANG II-stimulated increases in cardiomyocyte size. Quantitative real-time PCR analysis demonstrated that Nox2 is the homolog expressed at highest levels in primary neonatal cardiomyocytes, and small interference RNA (siRNA) directed against it selectively decreased Nox2 expression by >95% and abolished both ANG II-induced $O_2^-\cdot$ generation and cardiomyocyte hypertrophy. Finally, ANG II caused a time-dependent increase in Akt activity via activation of AT_1 receptors, and this response was abolished by Ad-mediated expression of cytosolic human $O_2^-\cdot$ dismutase (AdCu/ZnSOD). Furthermore, pretreatment of cardiomyocytes with dominant-negative Akt (AdDNAkt) abolished ANG II-induced cellular hypertrophy. These findings suggest that $O_2^-\cdot$ generated by a Nox2-containing NADPH oxidase is a central mediator of ANG II-induced Akt activation and cardiomyocyte hypertrophy, and that dysregulation of this signaling cascade may play an important role in cardiac hypertrophy.

superoxide radicals; renin-angiotensin system; dominant-negative Rac1; small interference RNA; oxidative stress

CARDIAC HYPERTROPHY is one of the most significant sequelae of ischemic heart disease, hypertension, and valvular disease (14). Initially an adaptive response that preserves cardiac output and minimizes wall tension, cardiac hypertrophy predisposes to ischemia, arrhythmia, and heart failure. Signal transduction pathways important in the pathogenesis of hypertrophy have been the target of many recent investigations, with angiotensin II (ANG II) emerging as a key molecule both in compensatory cardiac hypertrophy and in the pathogenesis of progressive myocardial dysfunction leading to heart failure (48, 54). Despite the importance of ANG II in cardiac hypertrophy, the signaling cascades downstream of ANG II receptor activation remain to be fully elucidated.

The small GTP-binding protein Rac1, a member of the Rho family of GTPases (51), has emerged as an important proximal molecule in the hypertrophic response induced by a variety of extracellular signals in cardiovascular cells (17). Hypertrophic agonists such as endothelin-1 and phenylephrine stimulate Rac1 activation in cultured cardiac myocytes (7), and adenovirus (Ad)-mediated expression of a dominant-negative (AdN17Rac1) or a constitutively active mutant of Rac1 (AdV12Rac1) has been shown to abolish or exacerbate, respectively, phenylephrine-induced hypertrophic responses (36). Transgenic mice expressing V12Rac1 specifically in myocardium develop dilated cardiac hypertrophy (50), and increased activation of Rac1 has been observed in left ventricles from patients with ischemic cardiomyopathy as well as dilated cardiomyopathy (29). In vascular smooth muscle cells (VSMC), ANG II has been shown to cause a rapid activation of Rac1 (39, 40), and AdN17Rac1 inhibits ANG II-induced hypertrophic signaling (40) in this cell type. There is some evidence that Rac1 plays a role in the ANG II-mediated hypertrophic response in cardiomyocytes (53), although the precise mechanisms are not fully understood.

The signaling pathways linking activated Rac1 and cellular hypertrophy may involve multiple molecules, although recent studies have focused on the participation of NADPH oxidase (6, 17, 29, 40). This oxidase is a multi-subunit enzyme composed of a membrane-bound heterodimeric subunit ($p22^{phox}$ and $gp91^{phox}$) and several cytoplasmic regulatory subunits including Rac1, $p47^{phox}$, and $p67^{phox}$ (4). Recently, several homologs of $gp91^{phox}$, termed the NADPH oxidase or Nox family of enzymes ($gp91^{phox}$ has been renamed Nox2), have been identified in several cardiovascular cell types including endothelial cells (26) and VSMC (24). These different homologs have been shown to play an agonist-specific role in regulation of reactive oxygen species (ROS) generation and cellular hypertrophy in these various cells (6). In VSMC, ANG II increases expression of Nox1, and a Nox1-containing NADPH oxidase is required for ANG II-induced ROS generation and hypertrophy (24, 49). Much less is known about the

Article published online before print. See web site for date of publication (http://physiolgenomics.physiology.org).

Address for reprint requests and other correspondence: R. L. Davisson, Dept. of Anatomy and Cell Biology, 1-418 Bowen Science Bldg., Roy J. and Lucille A. Carver College of Medicine, The Univ. of Iowa, Iowa City, IA 52242 (e-mail: robin-davisson@uiowa.edu).

Nox enzymes in cardiomyocytes, although one recent study (5) implicates Nox2 in ANG II-induced cardiac hypertrophy. However, because these in vivo studies utilized global knockout of Nox2, the role of this homolog in cardiomyocytes and the potential effect of compensatory increases in the expression of other Nox homologs in the heart and in other tissues are not known. Moreover, relative expression of the different Nox homologs in cardiomyocytes has not been established.

Activation of numerous growth-promoting signaling cascades in cardiomyocytes has been shown to require ROS (52). In particular, the serine-threonine kinase Akt (Akt) has been identified recently as a target of ROS and is a key downstream mediator of various agonists that cause cellular hypertrophy (55). Overexpression of a constitutively active mutant of Akt has been shown to increase cell surface area and expression of the cardiac hypertrophy marker atrial natriuretic peptide (ANP) (33, 37). In vivo, pressure overload leads to rapid activation of Akt in the myocardium, and these changes are correlated with increased cardiac hypertrophy (32). Furthermore, transgenic mice overexpressing Akt from a cardiomyocyte-specific promoter exhibit cardiac hypertrophy and enhanced myocardial contractility (22). However, a direct role of Akt signaling in ANG II/ROS-mediated cardiomyocyte hypertrophy has not been demonstrated.

Here we tested the hypothesis that Nox2-mediated superoxide ($O_2^-\cdot$) production and activation of Akt play a critical signaling role in ANG II-stimulated cardiomyocyte hypertrophy. We took advantage of the specificity of genetic approaches to inhibit cytoplasmic $O_2^-\cdot$ generation and Akt activation in primary rat neonatal cardiomyocytes. Our results show that *1*) blockade of Rac1 activation or inhibition of Nox2 expression by small interference RNA (si-Nox2) abolished both ANG II-stimulated ROS generation and cellular hypertrophy in primary neonatal rat cardiomyocytes, *2*) ANG II activates Akt through an $O_2^-\cdot$-dependent mechanism in cardiomyocytes, and *3*) Akt is a key regulator of ANG II-induced cardiomyocyte hypertrophy.

MATERIALS AND METHODS

Animals and Cardiomyocyte Cell Culture

Female Sprague-Dawley rats with pups (Harlan, Indianapolis, IN) were used. All protocols were approved by the University of Iowa Animal Care and Use Committee. The H9C2 cardiac myoblast cell line was purchased from the American Type Culture Collection (Manassas, VA) and cultured as described (20). Primary neonatal cardiomyocytes were dissociated from the hearts of 2-day-old rat pups (12–14 pups/culture) and cultured using the Neonatal Cardiomyocyte Isolation System (Worthington, Lakewood, NJ) as described (42). After two 30-min preplatings to reduce contamination with other cell types, myocytes were cultured in DMEM supplemented with 100 μmol/l bromodeoxyuridine (BrdU). Addition of BrdU has been shown to retard growth of cardiac fibroblasts (37). All experiments were performed after 24 h of incubation under serum-free conditions.

Recombinant Adenoviral Vectors

Construction and characterization of E1-deleted adenoviral vectors encoding human Cu/ZnSOD (AdCu/ZnSOD), HA-tagged dominant-negative Rac1 (AdN17Rac1), dominant-negative Akt in which alanine has been substituted for threonine^{308} and serine^{473} (AdDNAkt, HA-tagged), or the control vector (AdBgL II) have been described previously (2, 60, 62). Concentrations of virus that induce efficient gene transfer without cell death have been optimized previously (2, 15, 57, 60, 62). Appropriate subcellular compartment targeting of AdCu/ZnSOD also has been established (57). N17Rac, human Cu/ZnSOD, and DNAkt levels were determined by Western blot analysis as described (15, 57). Appropriate cytoplasmic targeting of AdCu/ZnSOD was verified by double immunostaining as described (57, 60). All gene transfer occurred 24 h before experimentation.

Measurement of Rac1 Activation

ANG II-stimulated activation of Rac1 was analyzed using the Rac Activation Assay Kit (Upstate, Charlottesville, VA) as described (60). Briefly, noninfected or AdN17Rac1- or AdBgL II-infected H9C2 cells were stimulated with vehicle, ANG II alone (5 or 30 min, 100 nmol/l), or ANG II subsequent to a 30-min pretreatment with the AT_1 receptor blocker losartan (100 μmol/l). GTP-bound Rac1 was separated using agarose beads conjugated to the p21 (Rac1)-binding domain, resolved by SDS-PAGE, and Western blot analysis was performed using an anti-Rac1 antibody. Relative band intensity was quantified using Quant Pro1 software (Bio-Rad).

Two-Dimensional Cell Surface Area Analysis

Two-dimensional (2-D) measurements of cardiomyocyte surface area were performed essentially by the method of Simpson (42). Briefly, primary cardiomyocytes were left untreated or were infected with AdBgL II, AdCu/ZnSOD, AdN17Rac1, or AdDNAkt for 24 h before treatment with vehicle, ANG II alone (100 nmol/l, 48 h), or ANG II subsequent to pretreatment with losartan (100 μmol/l, 30 min) for 48 h. After stimulation, cells were incubated with CellTracker Green (10 μmol/l, Molecular Probes) for 30 min, and fluorescent images were captured using a Zeiss LSM 510 laser confocal microscope. 2-D cell surface area was calculated for individual cells in each group using Image J analysis software (National Institutes of Health; NIH), and values are expressed as fold change relative to vehicle-treated cells.

3-D Cell Volume Analysis

Cardiomyocytes grown on chamber slides were treated as described above for 2-D analysis. After loading with CellTracker Green, cells were fixed in 3.7% paraformaldehyde for 30 min, coverslipped, and imaged using the Zeiss confocal microscope. A z-series of 2-D images for each cardiomyocyte was generated with a 1-μm interslice spacing as previously described (38). All images were loaded into Voxblast 3-D analysis software (Vaytek, Fairfield, IA) and reconstructed into 3-D images. 3-D volume for each cell was calculated as the sum of 2-D surface area measurements from all slices multiplied by the interslice distance. This sequence was repeated for all cells in each sample group. 3-D volume measurements are expressed as fold change relative to vehicle-treated cells.

Measurement of ROS Generation in Cardiomyocytes

Electron spin resonance spectroscopy. Electron spin resonance (ESR) studies were performed according to published methods (46) with minor modifications. Briefly, noninfected or AdN17Rac1-, AdCu/ZnSOD-, or AdBgL II-infected cardiomyocytes were collected by trypsin digestion and resuspended in HBSS containing 50 mmol/l spin trap 5,5-dimethyl-L-pyrroline-N-oxide (DMPO; Sigma). Cells were then stimulated with vehicle, ANG II (100 nmol/l), or ANG II after losartan pretreatment (100 μmol/l, 30 min), and ESR measurements were performed for 30 min using an X-band Bruker EMX spectrometer (Karlsruhe, Germany) at room temperature. Instrument settings were as follows: 1G modulation amplitude, 9.79-GHz microwave frequency, 100-kHz modulation frequency, 40-mW microwave power, 80 G/84 s scan rate, and 82-ms time constant. Hyperfine splitting constants were $a^N = a^H = 14.91$G, typical for the DMPO/

·OH spin adduct. Data are expressed as fold change relative to vehicle-treated cells.

Dihydroethidium fluorescence. The oxidant-sensitive fluoroprobe dihydroethidium (DHE) was used to measure O_2^-· levels in noninfected or AdCu/ZnSOD-, AdN17Rac1-, or AdBgL II-infected cardiomyocytes, as described (60, 61). Briefly, subconfluent cardiomyocytes were loaded with DHE (1 μmol/l, Molecular Probes) for 30 min before treatment with vehicle or ANG II (100 nmol/l). Fluorescent images were captured before and after 30 min of ANG II stimulation, using confocal microscopy. Fluorescence intensity was quantified in individual cells using Image J analysis software (NIH), as described (60), and expressed relative to pre-ANG II (0 min) values.

Quantitative Real-Time PCR Detection of Nox Homologs

Total RNA was isolated and reverse transcribed from rat primary cardiomyocytes and cardiac left ventricles. Quantitation of Nox1, Nox2, and Nox4 transcript levels was performed by amplification of cDNA prepared from total RNA with an ABI 7000 or 7700, using SYBR Green and primers specific for Nox1, Nox4, Nox2, and 18S mRNA. Primers were designed using Primer Express software (version 1.5, PE Biosystems, Foster City, CA), and were targeted to nonhomologous regions of the mRNA sequences of rat. All primers were synthesized by Integrated DNA Technologies (IDT, Coralville, IA). The primers used were as follows: Nox1 sense, 5′-CTACAGTAGAAGCCAACAGGCCAT-3′; Nox 1 anti-sense, 5′-ACTGTCACGTTTGGAGACTGGATG-3′; Nox2 sense, 5′-CCCTTTGGTACAGCCAGTGAAGAT-3′; Nox2 anti-sense, 5′-CAATCCCAGCTCCCACTAACATCA-3′; Nox4 sense, 5′-GGATCACAGAAGGTCCCTAGCAG-3′; and Nox4 anti-sense, 5′-GCAGCTACATGCACACCTGAGAA-3′.

Standard amplification conditions were utilized according to the manufacturer's specification (PE Biosystems). Quantification of Nox1, Nox4, and Nox2 mRNA levels in the samples was performed by calculating copy number from standard curves generated from pure templates as described previously (24). Data are expressed as transcript copy number relative to 18S copy number in a 100-ng total RNA sample.

Small Interference RNA Expression Plasmids

To accomplish intracellular expression of small interference RNA (siRNA), we designed short hairpin RNA (shRNA) constructs encoding inverted sequences of 21 base pairs with 3′-overhangs and separated by a six-nucleotide loop (5′-TATCGC). The shRNA cassette is designed such that, after annealing of two complementary oligos, the cassette has a 5′-blunt end and 3′-*Eco*RI cutting site for cloning into an expression plasmid (pacAd5CMV K-N pA, University of Iowa Vector Core). In this plasmid, the cytomegalovirus (CMV) promoter is used to drive expression of GFP as a reporter for siRNA expression. Downstream of this reporter, the shRNA constructs were cloned along with the U6 promoter to drive expression of shRNA in transfected cells. Each candidate shRNA clone was sequenced to verify that it retained 100% homology to Nox2. Initially, we tested three different shRNA sequences spaced throughout the mRNA of Nox2 (GenBank NM-023965) designed using general rules for siRNA selection described previously (13). In the initial screening, the most effective siRNA directed against Nox2 (5′-GAGTGGTGTGTGAATGCCAGA-3′) was located 370–390 bases (exon 5) from the start codon.

As a control, we have designed a random negative control siRNA (si-RNC) in collaboration with Integrated DNA Technologies (IDT, Coralville, Iowa). The DNA sequence for RNC, 5′-GGTTACCGCAACGAGGTTTGC-3′, was generated from random sequence generator software designed by the bioinformatics group at IDT. A sequence analysis pipeline was designed to first screen candidate sequences for similarity against the mouse transcriptome and then subsequently remove candidate sequences that contained similarity to sequences within the human, mouse, and rat genomes. First, 21 nucleotide-length candidate sequences were generated with equal probabilities of the 4 nucleotides. Second, these sequence fragments were aligned by the Smith Waterman algorithm with the *Mus musculus* mRNA library, the rna.fa.gz file downloaded from **ftp.ncbi.nlm.nih.gov/genomes/M_musculus/RNA/**. In ranking the candidate sequences by their longest contiguous ungapped match, three sequence fragments containing 14 contiguous matches were selected. To verify the mismatch properties, these three candidates were searched against the entire genome sequences from *Homo sapiens*, *M. musculus*, and *Rattus norvegicus* with basic local alignment search tool (BLAST) (1). The BLAST parameter of word size was set to 7 and the expectation value to 1,000.

siRNA Experiments

Primary cardiomyocytes were transfected with 6 μg of the appropriate plasmid using FuGENE 6 Transfection Reagent (Roche Diagnostics, Indianapolis, IN) for 72 h under serum-free conditions. To examine the effect of si-Nox2 on cardiomyocyte hypertrophy, cells were then stimulated with vehicle or ANG II for 48 h and loaded with CellTracker Red, and 2-D cell surface was measured as described above. For determination of the effect of si-Nox2 on ROS production, green fluorescent protein (GFP)-positive cardiomyocytes were first sorted by fluorescence-activated cell sorting (FACS, FACSDiVa; Becton Dickinson, Franklin Lakes, NJ). ROS levels in GFP-positive si-Nox2 or si-RNC expressing cardiomyocytes and nontransfected (GFP-negative) cardiomyocytes were determined by ESR as described above. The efficiency and selectivity of si-Nox2 was confirmed using real-time PCR as described above. To confirm the findings at the protein level, Western blotting was performed using an anti-Nox2 antibody (BD Biosciences, San Jose, CA) as described (3).

Measurement of Akt Kinase Activity

ANG II-stimulated activation of Akt in cardiomyocytes was analyzed using the Akt Kinase Assay Kit (Cell Signaling Technology, Beverly, MA) as described (15). Cardiomyocytes were stimulated with ANG II (100 nmol/l) for 0, 2, 5, and 10 min. In separate studies, Akt activation was determined in cardiomyocytes pretreated with the AT_1 receptor antagonist losartan (100 μmol/l, 30 min) or infected with AdDNAkt, AdCu/ZnSOD, or AdBgL II before stimulation with ANG II (10 min). Immunoprecipitated Akt was incubated with ATP and glycogen synthase kinase (GSK)-3α/β fusion protein, and Akt activity was determined by Western blot using an anti-phospho-GSK-3α/β antibody.

Statistical Analysis

Data are expressed as means ± SE and were analyzed by ANOVA (after Bartlett's test of homogeneity of variance), followed by the Newman-Keuls correction for multiple comparisons. Differences were considered significant at $P < 0.05$.

RESULTS

Ad-Mediated Expression of Dominant-Negative Rac1, Dominant-Negative Akt, and Human Cu/ZnSOD

To establish the optimal protocol for Ad-mediated expression of the Rac1 mutant (AdN17Rac1), dominant-negative Akt (AdDNAkt), and Cu/ZnSOD (AdCu/ZnSOD), the embryonic rat cardiac myoblast cell line H9C2 was used. As shown in the representative Western blot in Fig. 1*A*, infection of H9C2 cells with HA-tagged AdN17Rac1 ($n = 3$) resulted in a concentration-dependent increase in expression of N17Rac1, with 100 pfu/cell causing robust N17Rac1 expression in healthy cells.

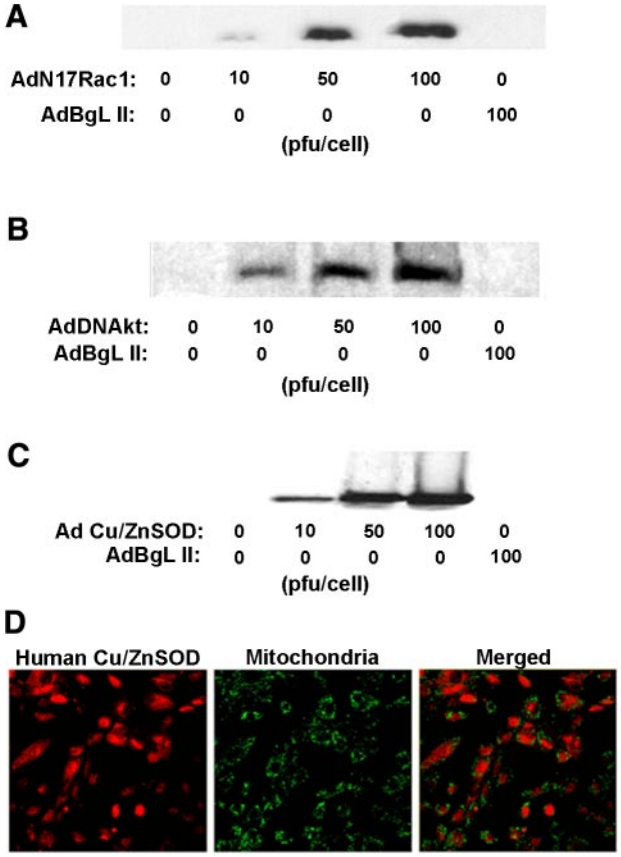

Fig. 1. Adenoviral (Ad)-mediated expression of dominant-negative Rac1, dominant-negative Akt, and human Cu/ZnSOD in cardiac cells. Representative Western blots demonstrating the expression of HA-tagged N17Rac1 (*A*; $n = 3$), HA-tagged dominant-negative Akt (*B*; $n = 3$), and human Cu/ZnSOD (*C*; $n = 4$) in cultured H9C2 cells infected with increasing concentrations of AdN17Rac1, AdDNAkt, AdCu/ZnSOD, or AdBgL II for 24 h. Antibodies used were anti-HA (*A* and *B*) and anti-human Cu/ZnSOD. *D*: representative photomicrographs ($n = 3$) showing cytoplasmic localization of human Cu/ZnSOD in cells infected with AdCu/ZnSOD (100 pfu/cell). After 24-h treatment with AdCu/ZnSOD, cells were stained for Cu/ZnSOD (red) and mitochondria (green). Lack of costaining (i.e., yellow) indicates cytoplasmic localization of Cu/ZnSOD.

Representative Western blots shown in Fig. 1, *B* and *C*, demonstrate that infection of cells with HA-tagged AdDNAkt ($n = 3$) and AdCu/ZnSOD ($n = 3$) resulted in concentration-dependent increases in expression of DNAkt and Cu/ZnSOD, respectively. It should be noted that 100 pfu/cell of AdDNAkt caused cell death in 10–20% of cells as indicated by remodeling and detachment of cells from the culture dishes, and so in all subsequent experiments, 50 pfu/cell of AdDNAkt and 100 pfu/cell of AdCu/ZnSOD and AdN17Rac1 were used. None of these proteins was observed in noninfected ($n = 3$) or AdBgL II-infected ($n = 3$) cells.

To demonstrate proper subcellular targeting of Cu/ZnSOD, double immunohistochemistry was performed. Infection of H9C2 cells with 100 pfu/cell of AdCu/ZnSOD resulted in gene transfer in >90% of cells. Appropriate localization to the cytoplasm was demonstrated by the lack of double labeling of human Cu/ZnSOD (red) and mitochondria (green) (i.e., no yellow staining in merged image) (Fig. 1*D*). This corroborates our earlier findings in other cell types (57).

AdN17Rac1 Abolishes ANG II-Induced Rac1 Activation and Cardiomyocyte Hypertrophy

To confirm the efficacy of the N17Rac1 mutant to inhibit ANG II-induced activation of Rac1, we measured Rac1 activity in ANG II-stimulated H9C2 cells. ANG II caused an increase in Rac1 activity by 5 min, and this was sustained for 30 min (Fig. 2*A*, *left*). AdN17Rac1 and losartan were equally

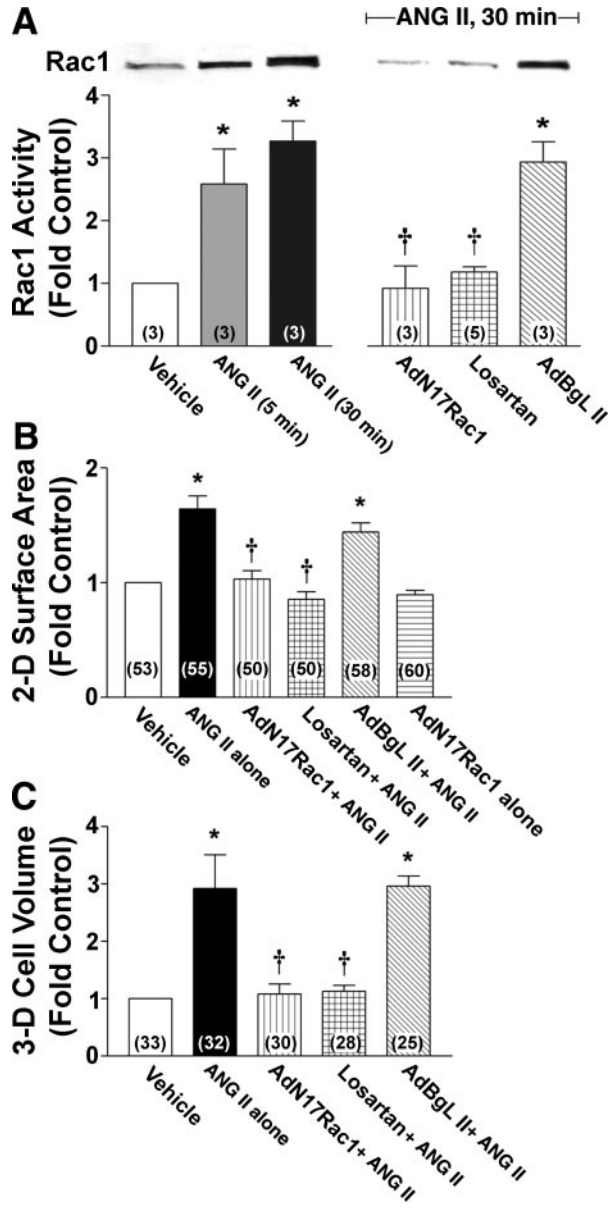

Fig. 2. AdN17Rac1 attenuates angiotensin II (ANG II)-induced Rac1 activation and cardiomyocyte hypertrophy. *A*: representative Western blots and summary data showing the time course of ANG II-stimulated Rac1 activation in H9C2 cardiomyoblasts (*left*) and inhibition of Rac1 activation at the 30-min time point by pretreatment with AdN17Rac1 or losartan (*right*). *B*: summary data showing ANG II-induced increases in cardiomyocyte 2-dimensional (2-D) cell surface area and inhibition of this response by AdN17Rac1 or losartan. *C*: summary data showing the effects of AdN17Rac1 or losartan on ANG II-stimulated increases in 3-D cell volume. Data in *B* and *C* are means ± SE (n in bars from 3–4 independent cultures) expressed relative to vehicle-treated cells. In all panels: $*P < 0.05$ vs. vehicle; $\dagger P < 0.05$ vs. ANG II alone and AdBgL II + ANG II.

effective at blocking the ANG II-induced increase in Rac1 activation at the 30-min time point, whereas infection of cells with AdBgL II had no effect on ANG II-stimulated Rac1 activation (Fig. 2*A*, *right*).

Having verified the effectiveness of AdN17Rac1 in blocking the ANG II-stimulated Rac1 activation, we next utilized this dominant-negative mutant to examine the role of Rac1 in ANG II-mediated hypertrophy in primary cardiomyocytes. In the first series of experiments, we determined the effect of AdN17Rac1 on 2-D cell surface area. Data from four separate experiments showed that 48-h stimulation with ANG II resulted in nearly a doubling of cardiomyocyte surface area compared with vehicle-treated cells (Fig. 2*B*). Expression of N17Rac1 virtually abolished the ANG II-induced increase in 2-D cell surface area, and the extent of inhibition was comparable with that produced by losartan pretreatment (Fig. 2*B*). Importantly, the hypertrophic response remained intact in AdBgL II-treated cells, confirming the specificity of AdN17Rac1. In addition, AdN17Rac1 alone did not have an effect on the surface area of unstimulated cardiomyocytes.

To confirm that increases in cell surface area reflect an increase in cell volume, we also performed a second series of experiments using 3-D analysis. As shown in the summary data in Fig. 2*C*, ANG II stimulation caused a threefold increase in cardiomyocyte volume relative to vehicle treatment. Similar to the 2-D studies, both AdN17Rac1 and losartan abolished this increase in 3-D cell volume, whereas AdBgL II-infected cells exhibited the same hypertrophic response to ANG II as noninfected cells (Fig. 2*C*).

AdN17Rac1 and AdCu/ZnSOD Attenuate ANG II-Stimulated ROS Generation in Cardiomyocytes

To determine whether ANG II-induced Rac1 activation is coupled to cardiomyocyte hypertrophy via activation of a ROS-generating NADPH oxidase, we next examined the effect of N17Rac1 on ANG II-stimulated increases in intracellular ROS generation in cardiomyocytes by ESR and DHE staining. As seen in the representative ESR tracings and summary data in Fig. 3*A*, treatment of cardiomyocytes with ANG II caused a threefold increase in ROS production compared with vehicle-treated cells. This response was significantly attenuated by pretreatment of cells with AdN17Rac1 or the AT_1 receptor antagonist losartan, but not by the control vector AdBgL II. Our findings that AdCu/ZnSOD also inhibited the ANG II-induced ESR signal (Fig. 3*A*) provide corroborative evidence that the free radical species involved is $O_2^-\cdot$. As further confirmation of this, the representative DHE fluorescence images and summary data presented in Fig. 3*B* demonstrate that AdN17Rac1 significantly attenuated ANG II-induced increases in $O_2^-\cdot$, whereas the response was unaffected by AdBgL II. Importantly, vehicle treatment had no effect on basal ROS generation over the 30-min time course of the study. As further verification of the specificity of the assay, pretreatment of cardiomyocytes with AdCu/ZnSOD virtually abolished the ANG II-induced increases in DHE staining (Fig. 3*B*). Taken together, these results suggest that a Rac1-regulated NADPH oxidase plays a central role in ANG II-stimulated $O_2^-\cdot$ generation in cardiomyocytes.

Abundance of Nox1, Nox2, and Nox4 Transcripts in Cardiomyocytes

Having established that a Rac1-regulated NADPH oxidase plays a critical role in ANG II-induced cardiomyocyte hypertrophy, we next sought to identify the predominant Nox homolog(s) comprising the oxidase in cardiomyocytes. Using quantitative real-time PCR, we compared the expression of Nox1, Nox2, and Nox4 in primary rat neonatal cardiomyocytes. Under basal conditions, Nox2 is most abundantly expressed, with Nox 4 at intermediate levels and Nox1 at very low but detectable levels in isolated cardiomyocytes (Fig. 4*A*). To compare this profile with the in vivo situation, real-time PCR experiments were also carried out in adult rat left ventricle (LV). Similar to isolated cardiomyocytes, Nox2 was expressed at significantly higher levels than Nox4 in these LV samples (133 ± 23 vs. 67 ± 12 copies/18S copies $\times 10^6$; $n = 3$, $P < 0.05$), while Nox1 levels were barely detectable (0.2 ± 0.03 copies/18S copies $\times 10^6$).

si-Nox2 Attenuates ANG II-Induced ROS Generation and Cardiomyocyte Hypertrophy

Because we found that Nox2 is the most abundant Nox homolog in cardiomyocytes, the next goal was to establish a functional role for this oxidase using siRNA to selectively inhibit Nox2 expression. First, to verify the specificity and effectiveness of si-Nox2, we performed quantitative real-time PCR on primary cardiomyocytes transfected with this reagent. Nox2 expression was decreased by >95% in cells treated with si-Nox2 compared with control si-RNC-treated cells (Fig. 4*B*). Importantly, si-Nox2 did not significantly alter expression of either Nox1 or Nox4 (si-Nox2 vs. si-RNC; Fig. 4*B*). In addition, Nox2 protein levels were nearly undetectable in si-Nox2-treated cultures compared with si-RNC (Fig. 4*C*), confirming the effectiveness of this siRNA in silencing Nox2 expression in cardiomyocytes.

To determine whether Nox2 is an important source of the ROS generated by ANG II in these cells, we compared ESR spectra in si-Nox2-transduced cells (GFP positive) with nontransduced (GFP-negative) cells from the same culture sample (after FACS). ANG II treatment caused a significant increase in ROS generation in si-Nox2-negative cardiomyocytes, whereas the si-Nox2-positive cardiomyocytes showed markedly attenuated ANG II-induced ROS generation (Fig. 5*A*). Further confirming specificity of si-Nox2-mediated inhibition, transfection of cardiomyocytes with the control si-RNC had no effect on the ANG II-stimulated increase in ROS production (Fig. 5*A*). These results confirm that a Nox2-containing NADPH oxidase is a key source of ANG II-induced ROS generation in cardiomyocytes.

Next, to establish a functional role for Nox2 in ANG II-induced cardiomyocyte hypertrophy, nontransfected cardiomyocytes (GFP negative) and cardiomyocytes transfected with si-Nox2 or si-RNC (GFP positive) were stimulated with ANG II for 48 h, and 2-D cell surface analyses were performed. As shown in the summary data in Fig. 5*B*, ANG II-induced increases in cardiomyocyte surface area were virtually abolished in cells treated with si-Nox2. In contrast, the ANG II-stimulated cardiomyocyte hypertrophy remained intact in cells transfected with the control plasmid si-RNC.

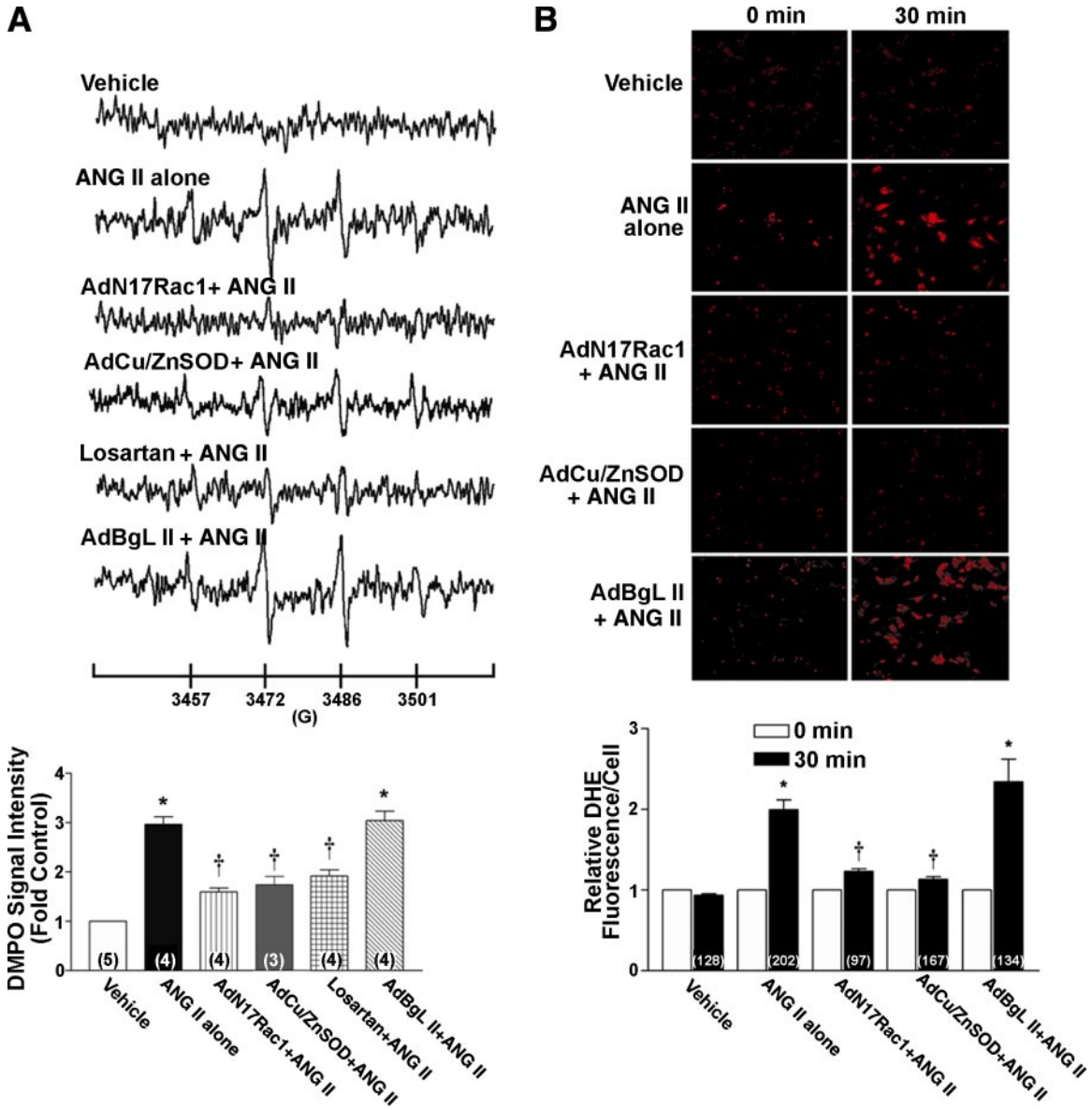

Fig. 3. AdN17Rac1 and AdCu/ZnSOD inhibit ANG II-induced reactive oxygen species (ROS) generation in cardiomyocytes. *A*: representative electron spin resonance (ESR) spectra (*top*) and summary data (*bottom*) showing inhibitory effects of AdN17Rac1, AdCu/ZnSOD, and losartan, but not AdBgL II, on ANG II-stimulated increases in ROS production in cardiomyocytes. Results are means ± SE (*n* in bars shows no. of independent cultures) and are expressed relative to vehicle-treated cells. *B*: representative photomicrographs (*top*) and summary data (*bottom*) demonstrating the effects of AdN17Rac1, AdCu/ZnSOD, and AdBgL II on ANG II-dependent increases in dihydroethidium (DHE) fluorescence in primary cardiomyocytes. Cells were imaged using confocal microscopy before (0 min) and after (30 min) stimulation with vehicle or ANG II, and DHE fluorescence was measured in individual cells. Data are means ± SE (*n* in bars shows no. of cells in 3–4 independent cultures) and are expressed relative to pre-ANG II stimulation (0 min) for each cell. Vehicle-treated cells served as a control. In all panels: $*P < 0.05$ vs. vehicle; †$P < 0.05$ vs. ANG II alone and AdBgL II + ANG II.

AdDNAkt and AdCu/ZnSOD Abolish ANG II-Induced Akt Activation and Cardiomyocyte Hypertrophy

To investigate the redox-sensitive pathways downstream of ANG II-induced Nox activation and ROS generation, we examined the role of Akt. This is an important signaling molecule in ANG II/ROS cascades involved in hypertrophy in other cell types (55). First, to determine the time course of Akt activation by ANG II and confirm the feasibility of using AdDNAkt to inhibit this pathway, we measured Akt activation by ANG II in primary cardiomyocytes. ANG II caused a rapid, time-dependent increase in Akt activity that was detectable after 2 min of stimulation, was significantly elevated by 5 min, and remained elevated through 10 min (Fig. 6*A*). AdDNAkt and losartan were equally effective at blocking the ANG II-stimulated increase in Akt activation (10 min), whereas infection of cells with the control virus AdBgL II had no effect on the Akt activation profile. These results show that ANG II stimulates Akt activation via AT_1 receptors and validate the use of AdDNAkt to investigate the role of Akt in ANG II signaling in cardiomyocytes.

Next, to determine the role of $O_2^-\cdot$ in ANG II-induced activation of Akt, we measured Akt kinase activity in cardiomyocytes pretreated with AdCu/ZnSOD. The representative Western blot and summary data shown in Fig. 6*B* demonstrate

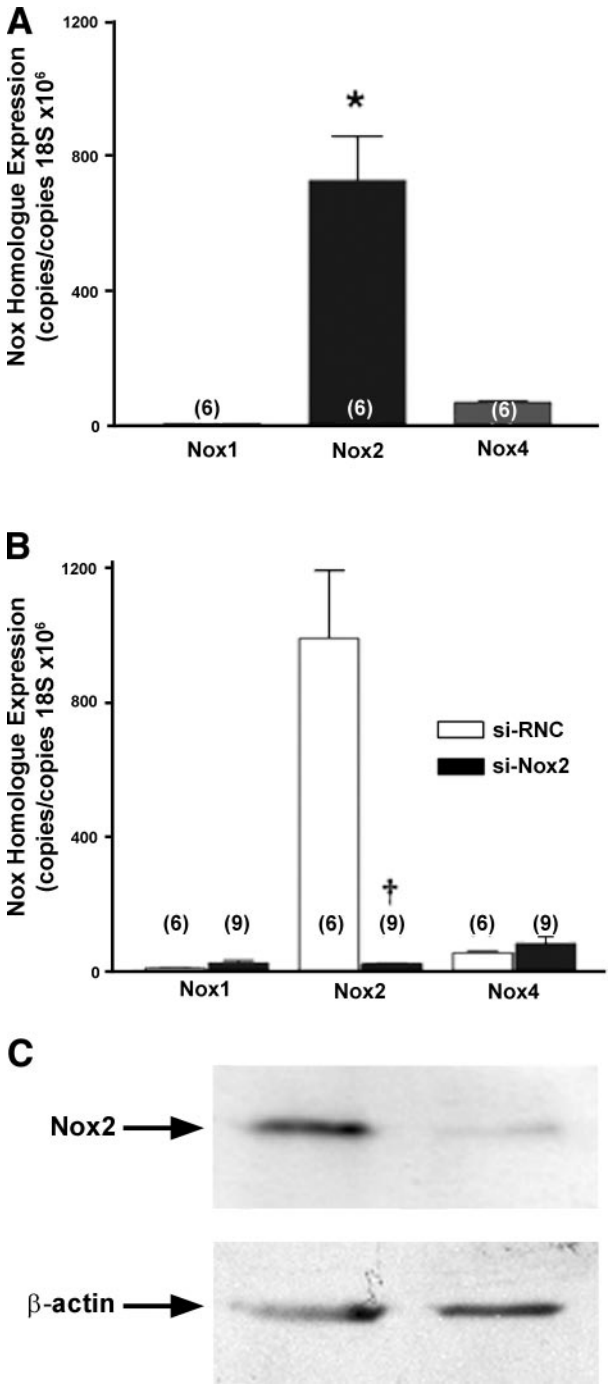

Fig. 4. Expression of different Nox homologs in rat primary cardiomyocytes and efficiency and selectivity of si-Nox2. *A*: summary real-time PCR data showing levels of Nox1, Nox2, and Nox4 mRNA in rat primary cardiomyocytes. *B*: real-time PCR data showing the effects of si-Nox2 and control si-RNC on Nox homolog expression. For both, copy nos. of Nox homologs were calculated from standard curves generated using purified Nox1, Nox2, and Nox4 cDNA and expressed relative to 18S mRNA. cDNA template equivalent to 100 ng of total RNA was used. Data are means ± SE (*n* in bars shows no. of independent cultures). *$P < 0.05$ vs. Nox1 and Nox4; †$P < 0.05$ vs. si-RNC. *C*: representative Western blots showing Nox2 protein levels in cardiomyocytes treated with si-Nox2 (*right*) compared with controls (*left*). Blots were stripped and reprobed for β-actin to control for equal sample loading. Data are representative of 2 separate cardiomyocyte cultures.

that ANG II-induced increases in Akt activity were significantly inhibited by AdCu/ZnSOD, whereas infection with AdBgL II had no effect. These results suggest that $O_2^-\cdot$ is a key upstream signaling molecule in the activation of Akt in cardiomyocytes.

Finally, to establish whether there are links between $O_2^-\cdot$ and Akt in ANG II-induced cardiomyocyte hypertrophy, we measured 2-D cell surface area in primary cardiomyocytes infected with either AdDNAkt or AdCu/ZnSOD. As shown in the summary data from three separate experiments in Fig. 7, both AdDNAkt and AdCu/ZnSOD significantly reduced the ANG II-stimulated increases in hypertrophy, whereas AdBgL II did not have any effect (Fig. 7). Importantly, neither AdDNAkt nor AdCuZnSOD alone significantly altered basal cardiomyocyte surface area (Fig. 7). Taken together, these results suggest that $O_2^-\cdot$-mediated activation of the Akt signaling cascade is required for ANG II-stimulated cardiomyocyte hypertrophy.

DISCUSSION

ANG II is a potent hypertrophic agent that regulates cardiomyocyte size and activates numerous growth-related signal transduction pathways (11, 48, 54). Here, using a variety of selective genetic reagents, we present evidence that $O_2^-\cdot$ radicals derived from a Rac1-activated, Nox2-containing NADPH oxidase play a key role in the proximal signaling cascade involved in ANG II-induced cardiomyocyte hypertrophy. Furthermore, Akt activation is downstream of $O_2^-\cdot$ generation in this pathway. The following evidence supports this conclusion: *1*) ANG II induced a rapid and robust activation of Rac1, an essential cofactor for agonist-stimulated assembly and activation of NADPH oxidase; this occurred in a time course that paralleled ROS production; *2*) pretreatment of cardiomyocytes with a dominant-negative isoform of Rac1 inhibited ANG II-dependent Rac1 activation, intracellular ROS production, and cardiomyocyte hypertrophy; *3*) targeted scavenging of cytoplasmic $O_2^-\cdot$ by Ad-mediated expression of cytosolic human Cu/ZnSOD markedly inhibited ANG II-induced increases in ROS production and cardiomyocyte hypertrophy; *4*) Nox2 homolog expression was greater than that of Nox4 in isolated cardiomyocytes and in adult LV tissue, while Nox1 expression was barely above the detection limit; *5*) siRNA-mediated inhibition of Nox2 expression in cardiomyocytes attenuated both ANG II-induced $O_2^-\cdot$ generation and cardiomyocyte hypertrophy; and *6*) ANG II induced $O_2^-\cdot$-dependent activation of Akt, and Ad-mediated expression of dominant-negative Akt abolished ANG II-induced cardiomyocyte hypertrophy.

Since the first report by Nakamura et al. (35) that nonspecific antioxidants inhibit ANG II-stimulated cardiomyocyte hypertrophy, a search has been underway to identify the cellular source(s) of ROS production involved in pathological hypertrophic signaling in the heart. Although early studies implicated both mitochondria (21) and xanthine oxidase (12) as sources of increased ROS, more recent studies suggest that NADPH oxidase may be the predominant source of ROS generation in the myocardium. Shah and colleagues (Li et al., Ref. 25) have shown increased expression of $p22^{phox}$, Nox2, $p67^{phox}$, and $p47^{phox}$ in the LV of aortic-banded guinea pigs. In the failing myocardium from patients with ischemic or dilated cardiomyopathy, an increase in Rac1 GTPase activity is associated with increased ROS production compared with healthy

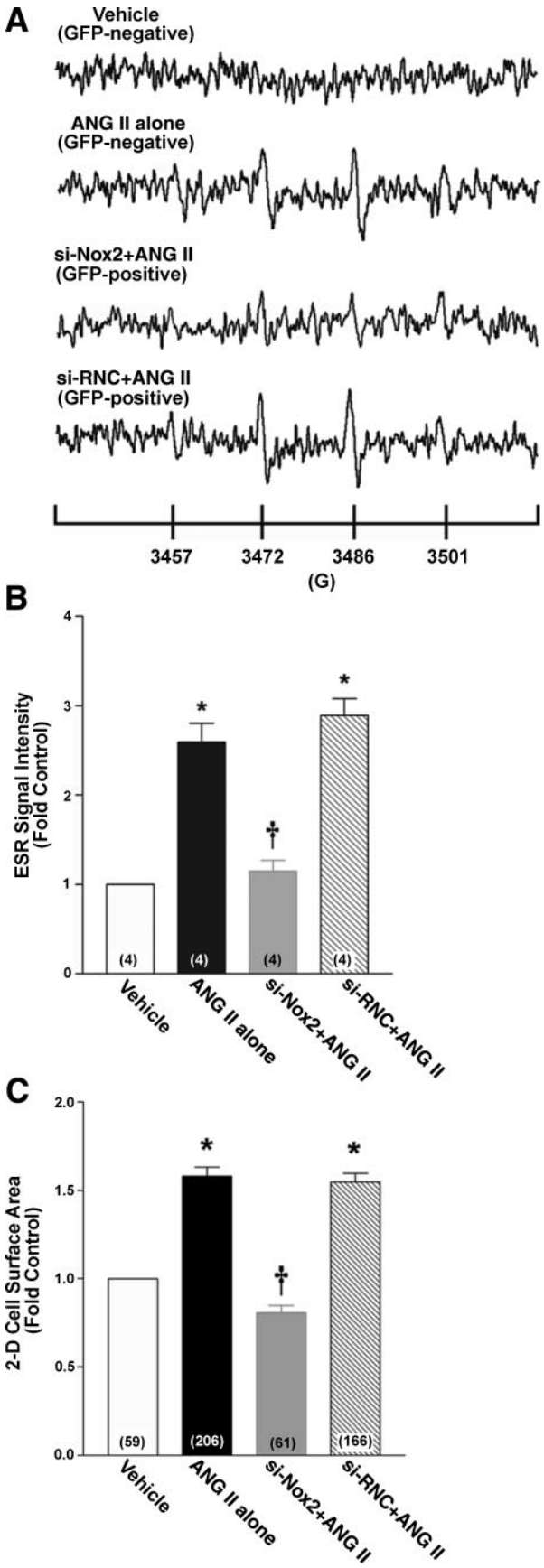

Fig. 5. si-Nox2 attenuates ANG II-induced ROS generation and cardiomyocyte hypertrophy. *A*: representative ESR tracings (*top*) and summary data (*bottom*) showing the effects of si-Nox2 or control plasmid si-RNC on ANG II-induced increases in ROS generation in cardiomyocytes. Responses in siRNA-transfected (GFP-positive) and nontransfected (GFP-negative) cells within the same culture were compared. Data are means ± SE (*n* in bars show no. of independent cultures) and are expressed relative to vehicle-treated cells. *B*: summary data showing effects of si-Nox2 and control siRNA (si-RNC) on ANG II-induced increase in 2-D cell surface area of cardiomyocytes. Cell Tracker Red was loaded into cells for cell perimeter enhancement to aid 2-D analysis. Data are means ± SE (*n* in bars from 4 independent cultures) and are expressed relative to vehicle-treated cells. In all panels: $*P < 0.05$ vs. vehicle; $\dagger P < 0.05$ vs. ANG II alone and si-RNC + ANG II.

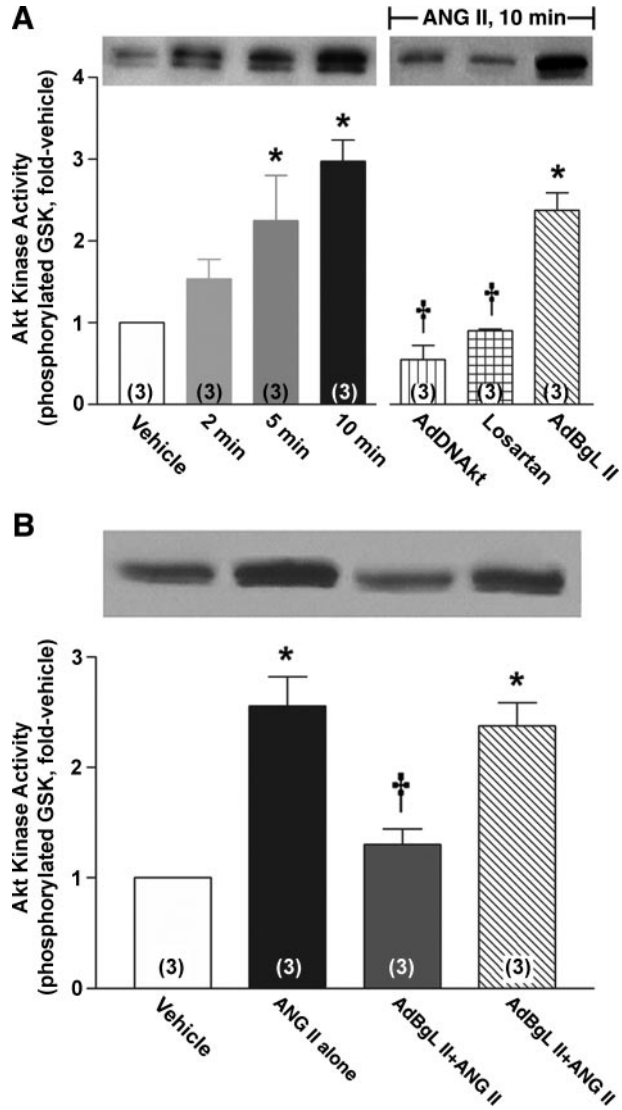

Fig. 6. AdDNAkt and AdCu/ZnSOD inhibit ANG II-induced Akt activation in cardiomyocytes. *A*: representative Western blot and summary data showing the time course of ANG II-stimulated increases in Akt kinase activity in primary cardiomyocytes (*left*) and inhibition of ANG II-induced (10-min) Akt activation by AdDNAkt and the AT_1 receptor antagonist losartan but not control virus AdBgL II (*right*). Data are means ± SE (*n* in bars shows no. of independent cultures) and are expressed relative to vehicle-treated cells. *B*: representative Western blot and summary data showing the effects of AdCu/ZnSOD and AdBgL II on Akt kinase activation in ANG II-stimulated cardiomyocytes (10 min). Data are means ± SE (*n* in bars shows no. of independent cultures) and are expressed relative to vehicle-treated cells. In all panels: $*P < 0.05$ vs. vehicle; $\dagger P < 0.05$ vs. ANG II alone (10 min) or AdBgL II + ANG II.

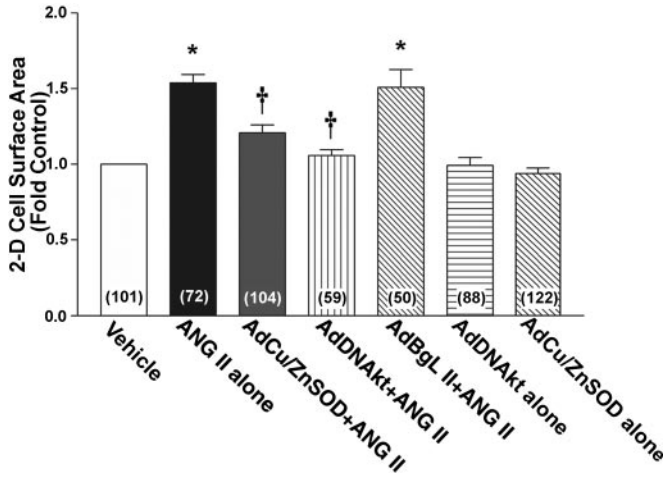

Fig. 7. AdDNAkt and AdCu/ZnSOD attenuate ANG II-induced increases in cardiomyocyte surface area. Summary data showing the inhibition of ANG II-induced cardiomyocyte hypertrophy by AdCu/ZnSOD or AdDNAkt. 2-D cell size of nonstimulated AdDNAkt- and AdCu/ZnSOD-infected cardiomyocytes was also measured. Data are means ± SE (n in bars from 3–4 independent cultures) and are expressed relative to vehicle-treated cells. *$P <$ 0.05 vs. vehicle; †$P < 0.05$ vs. ANG II alone or AdBgL II + ANG II.

hearts (29). Moreover, in animal models of hypertrophy-induced heart failure, as well as in ischemic and dilated cardiomyopathy, ROS levels are increased in cardiac tissue (10, 21, 45), and treatment with nonselective antioxidants has been shown to retard progression of LV hypertrophy and dysfunction (23, 30, 34). However, the full cascade linking ANG II, Rac1-regulated NADPH oxidase, ROS generation, and ultimately cardiomyocyte hypertrophy has not been definitively established. Using a cardiomyocyte cell culture model system and gene manipulation approaches, our results show that blockade of NADPH oxidase assembly and activity via dominant-negative Rac1 abolished both ANG II-induced $O_2^-\cdot$ generation and cardiomyocyte hypertrophy. Moreover, in complementary experiments where cytoplasm-targeted superoxide dismutase (SOD) was used to scavenge intracellular ROS, ANG II-induced cardiomyocyte hypertrophy was markedly attenuated. These results demonstrate that NADPH oxidase-mediated intracellular $O_2^-\cdot$ generation is a key regulator of ANG II-induced hypertrophy.

Extensive evidence from vascular studies suggests that endothelial cells, fibroblasts, and VSMC express the Nox homologs Nox1, Nox2, and Nox4 (47), but the levels of the different homologs and the regulation of their expression are cell type specific (24, 27). To identify the Nox homolog(s) comprising NADPH oxidase and mediating ANG II hypertrophic signaling in cardiomyocytes, we coupled quantitative PCR with an siRNA approach. We observed that Nox2 expression was greater than that of Nox4 in cultured cardiomyocytes, while Nox1 expression was barely detectable. Recently, two studies (5, 31) have shown that ROS generation and cardiac hypertrophy induced by systemic infusion of ANG II were attenuated in mice with gene-targeted deletion of Nox2. However, because of global gene deletion in these knockout mice and infiltration of NADPH oxidase-positive macrophages in the diseased myocardium, the precise identity of the Nox enzyme(s) mediating ANG II signaling in cardiac tissue remained unclear. Thus, to extend these studies, we used siRNA to selectively attenuate Nox2 expression in a cardiomyocyte culture system in vitro. Our results show that selective inhibition of Nox2 expression attenuated ANG II-induced ROS generation and cardiomyocyte hypertrophy. Together, these in vitro and in vivo studies demonstrate that Nox2 is required for ANG II-dependent cardiac hypertrophy.

Although we have taken precautions during cardiomyocyte isolation and culture to minimize contamination from cardiac nonmyocyte cells (see MATERIALS AND METHODS), it is possible that our myocyte cultures may contain some nonmyocytes. Indeed, previous studies (9, 43) using almost identical protocols for isolation and culture of neonatal rat cardiomyocytes report up to 10–15% nonmyocyte cells in myocyte cultures. Given the evidence that growth factors produced by nonmyocytes can lead to cardiomyocyte growth (28), and that nonmyocytes may express different complements of Nox homologs (18), further studies using pure cultures of cardiomyocytes by Percoll gradient centrifugation (19) will be needed to confirm the expression and function of different Nox homologs in ANG II-dependent cardiomyocyte hypertrophy.

Intensive investigation is currently focused on determining the identities of ROS mediating agonist-induced cellular hypertrophy. For example, in VSMC, Griendling and colleagues (Zafari et al., Ref. 58) have elegantly shown that hydrogen peroxide (H_2O_2) is a key ROS moiety in the hypertrophic signaling pathways utilized by ANG II. In cardiomyocytes, however, the identity of the ROS that mediate ANG II-stimulated hypertrophic signaling has not been clearly defined. A few studies in the myocardium have suggested that $O_2^-\cdot$ radicals may be playing a signaling role in cardiomyocyte hypertrophy. For example, Siwik et al. (44) were the first to show that inhibiting Cu/ZnSOD by the nonselective inhibitor diethyldithiocarbamic acid resulted in decreased protein synthesis and atrial natriuretic factor (ANF) expression in neonatal rat cardiomyocytes. Providing the first suggestion of a possible link between ANG II and $O_2^-\cdot$ specifically in cardiomyocytes, Nakagami et al. (34) demonstrated that polyethylene-glycol (PEG)-encapsulated SOD markedly inhibited ANG II-induced increases in cardiomyocyte protein synthesis and ANF secretion, whereas the H_2O_2 scavenger, a PEG-encapsulated catalase, had virtually no effect. However, because the subcellular localization of ROS scavenging by PEG-encapsulated SOD is unclear, and there was no evidence that PEG-encapsulated SOD inhibited cytoplasmic $O_2^-\cdot$ levels in this study, it was difficult to derive definitive conclusions. Therefore, to confirm that $O_2^-\cdot$ radicals are key signaling intermediates in ANG II-induced hypertrophic signaling, we utilized a genetic approach to manipulate intracellular $O_2^-\cdot$ levels. Our results show that selective scavenging of cytoplasmic $O_2^-\cdot$ with Ad-delivered Cu/ZnSOD markedly attenuated both ANG II-stimulated increases in cardiomyocyte size and intracellular $O_2^-\cdot$ levels. These results, combined with the previous studies discussed above, support the hypothesis that $O_2^-\cdot$ radicals mediate ANG II-stimulated hypertrophic signaling in cardiomyocytes. Further studies utilizing similar genetic approaches, but with Ad-GPx1 and Ad-catalase alone and in conjunction with Cu/ZnSOD, will be required to confirm this hypothesis.

One of the primary mechanisms by which ROS influence cellular function is through activation of redox-sensitive kinases and their downstream targets. In particular, phosphatidylinositide 3-kinase (PI3K)-Akt, p38MAPK, ERKs, and JNK

are activated by both oxidative stress and pressure overload in the myocardium (32, 56), and Akt has emerged as a key signaling molecule regulating cardiomyocyte survival and hypertrophy (56). Mice with cardiac-specific expression of constitutively active Akt spontaneously develop cardiac hypertrophy (22, 41). On the other hand, inactivation of Akt by dominant-negative Akt inhibits cardiomyocyte hypertrophy in vitro, induced by growth-promoting cytokines including tumor necrosis factor-α (TNF-α) (8), and constitutively active PI3K-induced cardiac hypertrophy in vivo (41). Griendling and colleagues (Ushio-Fukai et al., Ref. 55) provided the first evidence that ANG II activates Akt via ROS-mediated activation of PI3K, and that activated Akt is required for ANG II-induced hypertrophy in VSMC. In noncardiovascular cell types, ANG II activation of Akt was shown to be dependent on NADPH oxidase activation, as inhibition of this oxidase by expression of N17Rac1 or siRNA against Nox4 has been shown to markedly decrease Akt activity and cellular hypertrophy (16, 59). Our results support and extend these studies to cardiomyocytes by demonstrating that scavenging of $O_2^-\cdot$ with AdCu/ZnSOD significantly inhibited ANG II-stimulated increases in Akt activation. Interestingly, the extent of inhibition was similar to that observed with the AT_1 receptor antagonist losartan, suggesting a prominent role for ROS in Akt signaling in cardiomyocytes. Furthermore, our data show that pretreatment of cardiomyocytes with AdDNAkt abolished the ANG II-induced increase in cell surface area. Taken together, these data suggest that ANG II-stimulated increases in Nox2-mediated $O_2^-\cdot$ radical formation activate the Akt signaling pathway, and that this pathway plays a central role in cardiomyocyte hypertrophy.

It should be noted that cell surface area and volume measurements alone may not be sufficient as indexes of cardiomyocyte hypertrophy. Further studies using other indexes of cardiomyocyte hypertrophy, i.e., increases in protein synthesis and induction of fetal genes like ANF and β-myosin heavy chain (44), will be required to confirm the role of NADPH oxidase-derived ROS and Akt activation in ANG II-dependent cardiomyocyte hypertrophy. Future studies could be aimed at extending these studies using additional indexes of hypertrophy as well as identifying the targets of activated Akt in this hypertrophic response.

In summary, we have demonstrated that an increase in cytoplasmic $O_2^-\cdot$ generation by a Rac1-regulated Nox2 enzyme, with subsequent activation of Akt, plays a key role in ANG II-induced cardiomyocyte hypertrophy. We propose that low levels of $O_2^-\cdot$ might play an important role in regulating myocardial function under normal physiological conditions, but dysregulation of the cardiomyocyte redox state through an increase in Nox activity due to overactivation of the renin-angiotensin system is involved in the development of pathological cardiac hypertrophy by an Akt-dependent signaling cascade. As such, we speculate that therapeutic strategies targeting Nox2 in the heart may prove beneficial for the prevention of cardiac hypertrophic disease.

ACKNOWLEDGMENTS

We thank M. Zimmerman and D. Hoffmann for help in measuring ROS levels, P. Reimann for assistance with illustrations, and B. Knosp and S. Beck for help with Voxblast 3-D image analysis.

GRANTS

This study was supported by grants from the National Institutes of Health to R. L. Davisson (HL-55006) and J. F. Engelhardt (DK-51315). S. D. Hingtgen was supported by a Pre-Doctoral Minority Graduate Research Supplement to HL-6388 (R. L. Davisson). J. Yang was supported by an American Heart Association Post-Doctoral Fellowship.

REFERENCES

1. **Altschul SF, Gish W, Miller W, Myers EW, and Lipman DJ.** Basic local alignment search tool. *J Mol Biol* 215: 403–410, 1990.
2. **Anderson RD, Haskell RE, Xia H, Roessler BJ, and Davidson BL.** A simple method for the rapid generation of recombinant adenovirus vectors. *Gene Ther* 7: 1034–1038, 2000.
3. **Anrather J, Racchumi G, and Iadecola C.** NF-kappaB regulates phagocytic NADPH oxidase by inducing the expression of gp91phox. *J Biol Chem* 281: 5657–5667, 2006.
4. **Babior BM.** NADPH oxidase: an update. *Blood* 93: 1464–1476, 1999.
5. **Bendall JK, Cave AC, Heymes C, Gall N, and Shah AM.** Pivotal role of a gp91 (phox)-containing NADPH oxidase in angiotensin II-induced cardiac hypertrophy in mice. *Circulation* 105: 293–296, 2002.
6. **Byrne JA.** Contrasting roles of NADPH oxidase isoforms in pressure overload versus angiotensin II-induced cardiac hypertrophy. *Circ Res* 93: 802–804, 2003.
7. **Clerk A, Pham FH, Fuller SJ, Sahai E, Aktories K, Marais R, Marshall C, and Sugden PH.** Regulation of mitogen-activated protein kinases in cardiac myocytes through the small G protein Rac1. *Mol Cell Biol* 21: 1173–1184, 2001.
8. **Condorelli G, Morisco C, Latronico MV, Claudio PP, Dent P, Tsichlis P, Condorelli G, Frati G, Drusco A, Croce CM, and Napoli C.** TNF-alpha signal transduction in rat neonatal cardiac myocytes: definition of pathways generating from the TNF-alpha receptor. *FASEB J* 16: 1732–1737, 2002.
9. **Deng XF, Rokosh DG, and Simpson PC.** Autonomous and growth factor-induced hypertrophy in cultured neonatal mouse cardiac myocytes: comparison with rat. *Circ Res* 87: 781–788, 2000.
10. **Dhalla NS, Temsah RM, and Netticadan T.** Role of oxidative stress in cardiovascular diseases. *J Hypertens* 18: 655–673, 2000.
11. **Dostal DE, Hunt RA, Kule CE, Bhat GJ, Karoor V, McWhinney CD, and Baker KM.** Molecular mechanisms of angiotensin II in modulating cardiac function: intracardiac effects and signal transduction pathways. *J Mol Cell Cardiol* 29: 2893–2902, 1997.
12. **Ekelund UE, Harrison RW, Shokek O, Thakkar RN, Tunin RS, Senzaki H, Kass DA, Marban E, and Hare JM.** Intravenous allopurinol decreases myocardial oxygen consumption and increases mechanical efficiency in dogs with pacing-induced heart failure. *Circ Res* 85: 437–445, 1999.
13. **Elbashir SM, Harborth J, Weber K, and Tuschl T.** Analysis of gene function in somatic mammalian cells using small interfering RNAs. *Methods* 26: 199–213, 2002.
14. **Frey N and Olson EN.** Cardiac hypertrophy: the good, the bad, and the ugly. *Annu Rev Physiol* 65: 45–79, 2003.
15. **Fujio Y and Walsh K.** Akt mediates cytoprotection of endothelial cells by vascular endothelial growth factor in an anchorage-dependent manner. *J Biol Chem* 274: 16349–16354, 1999.
16. **Gorin Y, Ricono JM, Kim NH, Bhandari B, Choudhury GG, and Abboud HE.** Nox4 mediates angiotensin II-induced activation of Akt/protein kinase B in mesangial cells. *Am J Physiol Renal Physiol* 285: F219–F229, 2003.
17. **Gregg D, Rauscher FM, and Goldschmidt-Clermont PJ.** Rac regulates cardiovascular superoxide through diverse molecular interactions: more than a binary GTP switch. *Am J Physiol Cell Physiol* 285: C723–C734, 2003.
18. **Griendling KK.** Novel NAD (P)H oxidases in the cardiovascular system. *Heart* 90: 491–493, 2004.
19. **Harada M, Saito Y, Kuwahara K, Ogawa E, Ishikawa M, Nakagawa O, Miyamoto Y, Kamitani S, Hamanaka I, Kajiyama N, Takahahi N, Masuda I, Itoh H, and Nakao K.** Interaction of myocytes and nonmyocytes is necessary for mechanical strech to induce ANP/BNP production in cardiocyte culture. *J Cardiovasc Pharmacol* 31, *Suppl* 1: S357–S359, 1998.
20. **Hescheler J, Meyer R, Plant S, Krautwurst D, Rosenthal W, and Schultz G.** Morphological, biochemical, and electrophysiological charac-

terization of a clonal cell (H9c2) line from rat heart. *Circ Res* 69: 1476–1486, 1991.
21. **Ide T, Tsutsui H, Kinugawa S, Suematsu N, Hayashidani S, Ichikawa K, Utsumi H, Machida Y, Egashira K, and Takeshita A.** Direct evidence for increased hydroxyl radicals originating from superoxide in the failing myocardium. *Circ Res* 86: 152–157, 2000.
22. **Kim YK, Kim SJ, Yatani A, Huang Y, Castelli G, Vatner DE, Liu J, Zhang Q, Diaz G, Zieba R, Thaisz J, Drusco A, Croce C, Sadoshima J, Condorelli G, and Vatner SF.** Mechanism of enhanced cardiac function in mice with hypertrophy induced by overexpressed Akt. *J Biol Chem* 278: 47622–47628, 2003.
23. **Kinugawa S, Tsutsui H, Hayashidani S, Ide T, Suematsu N, Satoh S, Utsumi H, and Takeshita A.** Treatment with dimethylthiourea prevents left ventricular remodeling and failure after experimental myocardial infarction in mice: role of oxidative stress. *Circ Res* 87: 392–398, 2000.
24. **Lassegue B, Sorescu D, Szocs K, Yin Q, Akers M, Zhang Y, Grant SL, Lambeth JD, and Griendling KK.** Novel gp91 (phox) homologues in vascular smooth muscle cells: nox1 mediates angiotensin II-induced superoxide formation and redox-sensitive signaling pathways. *Circ Res* 88: 888–894, 2001.
25. **Li JM, Gall NP, Grieve DJ, Chen M, and Shah AM.** Activation of NADPH oxidase during progression of cardiac hypertrophy to failure. *Hypertension* 40: 477–484, 2002.
26. **Li JM and Shah AM.** Intracellular localization and preassembly of the NADPH oxidase complex in cultured endothelial cells. *J Biol Chem* 277: 19952–19960, 2002.
27. **Liu J, Ormsby A, Oja-Tebbe N, and Pagano PJ.** Gene transfer of NAD (P)H oxidase inhibitor to the vascular adventitia attenuates medial smooth muscle hypertrophy. *Circ Res* 95: 587–594, 2004.
28. **Long CS, Henrich CJ, and Simpson PC.** A growth factor for cardiac myocytes is produced by cardiac nonmyocytes. *Cell Regul* 2: 1081–1095, 1991.
29. **Maack C, Kartes T, Kilter H, Schafers HJ, Nickenig G, Bohm M, and Laufs U.** Oxygen free radical release in human failing myocardium is associated with increased activity of rac1-GTPase and represents a target for statin treatment. *Circulation* 108: 1567–1574, 2003.
30. **MacCarthy PA, Grieve DJ, Li JM, Dunster C, Kelly FJ, and Shah AM.** Impaired endothelial regulation of ventricular relaxation in cardiac hypertrophy: role of reactive oxygen species and NADPH oxidase. *Circulation* 104: 2967–2974, 2001.
31. **Maytin M, Siwik DA, Ito M, Xiao L, Sawyer DB, Liao R, and Colucci WS.** Pressure overload-induced myocardial hypertrophy in mice does not require gp91phox. *Circulation* 109: 1168–1171, 2004.
32. **Miyamoto T, Takeishi Y, Takahashi H, Shishido T, Arimoto T, Tomoike H, and Kubota I.** Activation of distinct signal transduction pathways in hypertrophied hearts by pressure and volume overload. *Basic Res Cardiol* 99: 328–337, 2004.
33. **Morisco C, Zebrowski D, Condorelli G, Tsichlis P, Vatner SF, and Sadoshima J.** The Akt-glycogen synthase kinase 3beta pathway regulates transcription of atrial natriuretic factor induced by beta-adrenergic receptor stimulation in cardiac myocytes. *J Biol Chem* 275: 14466–14475, 2000.
34. **Nakagami H, Takemoto M, and Liao JK.** NADPH oxidase-derived superoxide anion mediates angiotensin II-induced cardiac hypertrophy. *J Mol Cell Cardiol* 35: 851–859, 2003.
35. **Nakamura K, Fushimi K, Kouchi H, Mihara K, Miyazaki M, Ohe T, and Namba M.** Inhibitory effects of antioxidants on neonatal rat cardiac myocyte hypertrophy induced by tumor necrosis factor-alpha and angiotensin II. *Circulation* 98: 794–799, 1998.
36. **Pracyk JB, Tanaka K, Hegland DD, Kim KS, Sethi R, Rovira II, Blazina DR, Lee L, Bruder JT, Kovesdi I, Goldshmidt-Clermont PJ, Irani K, and Finkel T.** A requirement for the rac1 GTPase in the signal transduction pathway leading to cardiac myocyte hypertrophy. *J Clin Invest* 102: 929–937, 1998.
37. **Purcell NH, Tang G, Yu C, Mercurio F, DiDonato JA, and Lin A.** Activation of NF-kappa B is required for hypertrophic growth of primary rat neonatal ventricular cardiomyocytes. *Proc Natl Acad Sci USA* 98: 6668–6673, 2001.
38. **Sanlioglu S, Benson PK, Yang J, Atkinson EM, Reynolds T, and Engelhardt JF.** Endocytosis and nuclear trafficking of adeno-associated virus type 2 are controlled by rac1 and phosphatidylinositol-3 kinase activation. *J Virol* 74: 9184–9196, 2000.
39. **Schmitz U, Thommes K, Beier I, Wagner W, Sachinidis A, Dusing R, and Vetter H.** Angiotensin II-induced stimulation of p21-activated kinase and c-Jun NH2-terminal kinase is mediated by Rac1 and Nck. *J Biol Chem* 276: 22003–22010, 2001.
40. **Seshiah PN, Weber DS, Rocic P, Valppu L, Taniyama Y, and Griendling KK.** Angiotensin II stimulation of NAD (P)H oxidase activity: upstream mediators. *Circ Res* 91: 406–413, 2002.
41. **Shioi T, McMullen JR, Kang PM, Douglas PS, Obata T, Franke TF, Cantley LC, and Izumo S.** Akt/protein kinase B promotes organ growth in transgenic mice. *Mol Cell Biol* 22: 2799–2809, 2002.
42. **Simpson P.** Stimulation of hypertrophy of cultured neonatal rat heart cells through an alpha 1-adrenergic receptor and induction of beating through an alpha 1- and beta 1-adrenergic receptor interaction. Evidence for independent regulation of growth and beating. *Circ Res* 56: 884–894, 1985.
43. **Simpson P and Savion S.** Differentiation of rat myocytes in single cell cultures with and without proliferating nonmyocardial cells. Cross-striations, ultrastructure, and chronotropic response to isoproterenol. *Circ Res* 50: 101–116, 1982.
44. **Siwik DA, Tzortzis JD, Pimental DR, Chang DL, Pagano PJ, Singh K, Sawyer DB, and Colucci WS.** Inhibition of copper-zinc superoxide dismutase induces cell growth, hypertrophic phenotype, and apoptosis in neonatal rat cardiac myocytes in vitro. *Circ Res* 85: 147–153, 1999.
45. **Sorescu D and Griendling KK.** Reactive oxygen species, mitochondria, and NAD (P)H oxidases in the development and progression of heart failure. *Congest Heart Fail* 8: 132–140, 2002.
46. **Sorescu D, Somers MJ, Lassegue B, Grant S, Harrison DG, and Griendling KK.** Electron spin resonance characterization of the NAD (P)H oxidase in vascular smooth muscle cells. *Free Radic Biol Med* 30: 603–612, 2001.
47. **Sorescu D, Weiss D, Lassegue B, Clempus RE, Szocs K, Sorescu GP, Valppu L, Quinn MT, Lambeth JD, Vega JD, Taylor WR, and Griendling KK.** Superoxide production and expression of nox family proteins in human atherosclerosis. *Circulation* 105: 1429–1435, 2002.
48. **Sugden PH and Clerk A.** Cellular mechanisms of cardiac hypertrophy. *J Mol Med* 76: 725–746, 1998.
49. **Suh YA, Arnold RS, Lassegue B, Shi J, Xu X, Sorescu D, Chung AB, Griendling KK, and Lambeth JD.** Cell transformation by the superoxide-generating oxidase Mox1. *Nature* 401: 79–82, 1999.
50. **Sussman MA, Welch S, Walker A, Klevitsky R, Hewett TE, Price RL, Schaefer E, and Yager K.** Altered focal adhesion regulation correlates with cardiomyopathy in mice expressing constitutively active rac1. *J Clin Invest* 105: 875–886, 2000.
51. **Symons M and Settleman J.** Rho family GTPases: more than simple switches. *Trends Cell Biol* 10: 415–419, 2000.
52. **Takano H, Zou Y, Hasegawa H, Akazawa H, Nagai T, and Komuro I.** Oxidative stress-induced signal transduction pathways in cardiac myocytes: involvement of ROS in heart diseases. *Antioxid Redox Signal* 5: 789–794, 2003.
53. **Takemoto M, Node K, Nakagami H, Liao Y, Grimm M, Takemoto Y, Kitakaze M, and Liao JK.** Statins as antioxidant therapy for preventing cardiac myocyte hypertrophy. *J Clin Invest* 108: 1429–1437, 2001.
54. **Unger T.** The role of the renin-angiotensin system in the development of cardiovascular disease. *Am J Cardiol* 89: 3A–9A, 2002.
55. **Ushio-Fukai M, Alexander RW, Akers M, Yin Q, Fujio Y, Walsh K, and Griendling KK.** Reactive oxygen species mediate the activation of Akt/protein kinase B by angiotensin II in vascular smooth muscle cells. *J Biol Chem* 274: 22699–22704, 1999.
56. **Vlahos CJ, McDowell SA, and Clerk A.** Kinases as therapeutic targets for heart failure. *Nat Rev Drug Discov* 2: 99–113, 2003.
57. **Yang J, Marden JJ, Fan C, Sanlioglu S, Weiss RM, Ritchie TC, Davisson RL, and Engelhardt JF.** Genetic redox preconditioning differentially modulates AP-1 and NF kappa B responses following cardiac ischemia/reperfusion injury and protects against necrosis and apoptosis. *Mol Ther* 7: 341–353, 2003.
58. **Zafari AM, Ushio-Fukai M, Akers M, Yin Q, Shah A, Harrison DG, Taylor WR, and Griendling KK.** Role of NADH/NADPH oxidase-derived H2O2 in angiotensin II-induced vascular hypertrophy. *Hypertension* 32: 488–495, 1998.
59. **Zeng L, Xu H, Chew TL, Chisholm R, Sadeghi MM, Kanwar YS, and Danesh FR.** Simvastatin modulates angiotensin II signaling pathway by preventing Rac1-mediated upregulation of p27. *J Am Soc Nephrol* 15: 1711–1720, 2004.

60. **Zimmerman MC, Dunlay RP, Lazartigues E, Zhang Y, Sharma RV, Engelhardt JF, and Davisson RL.** Requirement for Rac1-dependent NADPH oxidase in the cardiovascular and dipsogenic actions of angiotensin II in the brain. *Circ Res* 95: 532–539, 2004.
61. **Zimmerman MC, Lazartigues E, Lang JA, Sinnayah P, Ahmad IM, Spitz DR, and Davisson RL.** Superoxide mediates the actions of angiotensin II in the central nervous system. *Circ Res* 91: 1038–1045, 2002.
62. **Zwacka RM, Zhou W, Zhang Y, Darby CJ, Dudus L, Halldorson J, Oberley L, and Engelhardt JF.** Redox gene therapy for ischemia/reperfusion injury of the liver reduces AP1 and NF-kappaB activation. *Nat Med* 4: 698–704, 1998.